Accepted Manuscript online: 2021-04-01 Article published online: 2021-05-26

Influence of the Location of Electron-Donating 3,4-Ethylenedioxythiophene (EDOT) Moiety in the A–π–D–π–A Type Conjugated Molecules on the Optoelectronic Properties and Photovoltaic Performances

Lilei Wang[a,b]
Ying Zhang[c]
Xiang Guan[a]
Wei Gao[a]
Yi Lin[d]
Qun Luo[a]
Hongwei Tan[c]
Hai-Bo Yang*[b]
Chang-Qi Ma*[a]

[a] Printable Electronics Research Center, Suzhou Institute of Nano-Tech and Nano-Bionics (SINANO), Chinese Academy of Sciences, 398 Ruo Shui Road, SEID SIP, Suzhou, Jiangsu, 215123, P. R. China
[b] Department of Chemistry, Shanghai Key Laboratory of Green Chemistry and Chemical, East China Normal University, 3663 North Zhongshan Road, Shanghai 200062, P. R. China
[c] College of Chemistry, Beijing Normal University, 19 XinJieKouWai Street, HaiDian District Beijing 100875, P. R. China
[d] Department of Chemistry, Xi'an Jiaotong Liverpool University, 111 Ren Ai Road, SEID SIP, Suzhou, Jiangsu, 215123, P. R. China
hbyang@chem.ecnu.edu.cn; cqma2011@sinano.ac.cn

Dedication to Prof. Peter Bäuerle on the occasion of his 65th birthday.

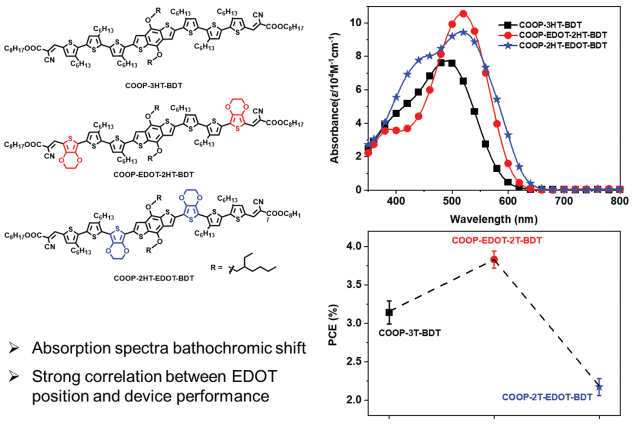

Received: 11.02.2021
Accepted after revision: 16.03.2021
DOI: 10.1055/a-1472-7109; Art ID: om-21-0020oa

Abstract A–π–D–π–A type conjugated small molecules play an indispensable role in organic photovoltaics. Understanding the relationship between the molecular structure and performance is a fundamental question for the further rational design of high-performance organic materials. To red-shift the absorption spectrum of benzo[1,2-*b*:4,5-*b*']dithiophene (BDT) based A–π–D–π–A type compounds, an electron-donating 3,4-ethylenedioxythiophene (EDOT) moiety was introduced into the π-conjugation bridge unit. Two new compounds with EDOT next to the central BDT core (**COOP-2HT-EDOT-BDT**) or next to the terminal electron acceptor unit (**COOP-EDOT-2HT-BDT**) were synthesized and characterized. The compound **COOP-2HT-EDOT-BDT** showed higher molar extinction coefficient ($\varepsilon_{abs}^{max} = 1.06 \times 10^5$ L mol^{-1} cm^{-1}), lower optical band gap (E_g = 1.56 eV) and high HOMO energy level ($E_{HOMO} = -5.08$ eV) than **COOP-EDOT-2HT-BDT** ($\varepsilon_{abs}^{max} = 0.96 \times 10^5$ L mol^{-1} cm^{-1}, E_g = 1.71 eV, $E_{HOMO} = -5.26$ eV), which is attributed to the intensive interaction between the EDOT unit and the HOMO orbital, as confirmed by the theoretical calculation results. However, the higher power conversion efficiency of 3.58% was achieved for the **COOP-EDOT-2HT-BDT**: $PC_{61}BM$-based solar cells, demonstrating that the electron-donating EDOT unit adjacent to the electron-withdrawing end-capped group (COOP) is a better way to achieve high-performance photovoltaic materials.

Key words organic solar cells, organic semiconductors, A–π–D–π–A small molecules, benzo[1,2-*b*:4,5-*b*']dithiophene derivatives, 3,4-ethylenedioxythiophene

Introduction

Solution-processed small molecules show advantages of well-defined structures, easy modification and purification, good batch-to-batch reproducibility and potential high power conversion efficiency (PCE) in organic solar cells.[1] Small molecules based on the benzo[1,2-*b*:4,5-*b*']dithiophene (BDT) core received great attention due to the planarity of the BDT moiety, high charge carrier mobility and outstanding photovoltaic performances of its derivatives.[2] Three different ways were applied to functionalize the molecular structures based on BDT: structure modification on the 4,8-position of the BDT-core unit,[3] tuning structure of the end-capped acceptor moiety,[4] and changing the π-conjugation bridge

unit.[5] Both optoelectronic property and photovoltaic performance can be tuned through these molecular structure modification and high PCE of over 15% was reported for this type of organic materials.[6]

3,4-Ethylenedioxythiophene (EDOT) is one of the most widely used π-conjugated electron-donating building blocks for functional π-conjugated polymers and small molecules.[7] Introducing EDOT unit into the π-conjugation chain generally leads to a red-shift of the absorption band and reduction of the optical band gap, which would be beneficial for application in solar cells.[8] For example, Langa et al. reported the introduction of an EDOT unit to oligo-thienylenevinylene compounds, which leads to a large red-shift of absorption band to 610–650 nm, and a PCE of 4.9% was reported for a solar cell using a rhodamine-terminated oligothienylenevinylene (SM06) as the electron donor.[9] While Jenekhe et al. reported the cooperation of EDOT into a perylene diimide (PDI) dimer as the conjugated linker, which leads to a broad absorption band over 500–730 nm. This EDOT-containing PDI dimer was used as the electron acceptor in polymer solar cells, and a high PCE of 8.5% was achieved when blended with conjugated polymers.[10] Also, Qiao et al. demonstrated that incorporation of an EDOT unit into the triphenylamine derivative ensures good planarity of the molecule M104, which improves the hole mobility of the materials and the consequent PCE of the perovskite solar cells.[11] On the other hand, BDT-based A–π–D–π–A small molecules are among the most efficient organic semiconductors in organic solar cells, further red-shifting the absorption band would be beneficial for use in solar cells. Therefore, it is highly interesting to introduce the EDOT unit into these types of molecules and understand the substitution effect of the EDOT unit. Herein, we report the synthesis of two novel BDT-cored A–π–D–π–A molecules **COOP-2HT-EDOT-BDT** and **COOP-EDOT-2HT-BDT**, where the EDOT unit is next to the core BDT unit or the terminal COOP moiety, respectively. Optical and electrochemical properties of these two compounds were investigated and compared to those of the reference compound **COOP-3HT-BDT** (Scheme 1). Results showed that both EDOT-functionalized compounds showed red-shifted absorption bands and smaller optical band gaps. However, the introduction of EDOT next to the BDT core unit lowers photovoltaic performance due to the increasing HOMO energy level, whereas introducing the EDOT unit next to the terminal electron acceptor unit increases device performance, which has a balanced red-shift of absorption band and less influenced HOMO energy level. The current work provides a useful guideline for further development of conjugated organic small molecules for organic solar cells.

Results and Discussion

Synthesis

The strategy for preparation of these two molecules with different positions of EDOT is outlined in Scheme 1. The building blocks **EDOT-Bp**,[12] **CHO-2HT-Br**,[13] **CHO-EDOT-Br**,[14] and **Sn-HT**[15] were synthesized according to the literature. Suzuki coupling of **EDOT-Bp** and **CHO-2HT-Br** catalyzed by $Pd_2(dba)_3{\cdot}CHCl_3$ catalyst afforded the desired compound **CHO-2HT-EDOT** in a yield of 88%. Compound **CHO-2HT-EDOT-Br** was prepared by bromination of **CHO-2HT-EDOT**

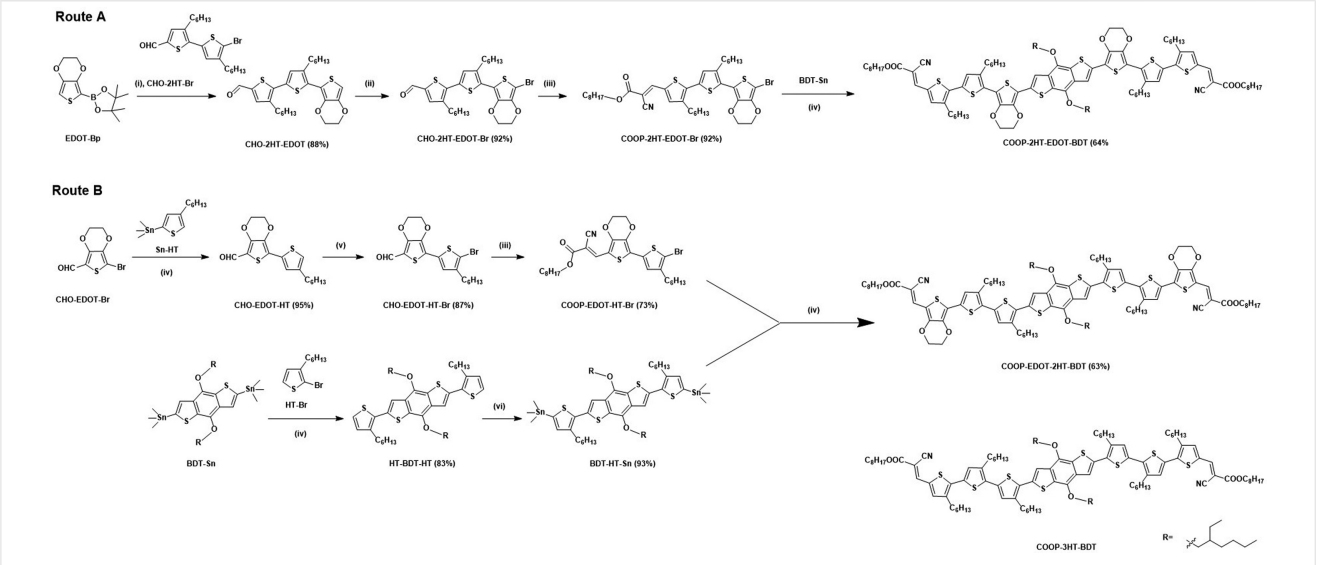

Scheme 1 Synthetic routes to the target molecules: (i) $Pd_2(dba)_3{\cdot}CHCl_3$, $HP(t\text{-}Bu)_3{\cdot}BF_4$, K_2CO_3 (1 M), THF, r. t.; (ii) NBS, THF, AcOH, 0 °C to r. t.; (iii) octyl 2-cyanoacetate, piperidine, dry $CHCl_3$; (iv) $Pd(pph_3)_4$, DMF, 80 °C; (v) NBS, THF, −20 °C; (vi) *n*-BuLi, −78 °C (30 min) to r. t. (30 min) then Me_3SnCl, −78 °C to r. t.

with NBS in THF in a 92% yield. And then, octyl 2-cynoacetate and piperidine were used to get compound **COOP-2HT-EDOT-Br** as a dark red solid in a high yield of 92%. The title compound **COOP-2HT-EDOT-BDT** was obtained in a moderate 64% yield by a Stille coupling of **COOP-2HT-EDOT-Br** with **BDT-Sn** using $Pd(PPh_3)_4$ as a catalyst (route A). The target molecule **COOP-EDOT-2HT-BDT** was obtained by Stille cross-coupling of **CHO-EDOT-HT-Br** and **BDT-HT-Sn** (route B) in a yield of 63%. Chemical structures of all new compounds were fully characterized by ^{1}H NMR, ^{13}C NMR and mass spectrometry (see the Supporting Information, Figures S1–S4). More synthesis details are also presented in the Experimental Section. Synthesis of the reference compound **COOP-3HT-BDT** was reported in our previous paper.[5a] Both of the two target molecules show reasonable thermal properties characterized by thermogravimetric analysis measurement in a nitrogen atmosphere (Figure S5). The decomposition temperatures determined from the 5% weight loss were 349 °C and 340 °C for **COOP- EDOT-2HT-BDT** and **COOP-2HT-EDOT-BDT**, respectively.

Photophysical Properties

These compounds' UV-vis absorption spectra were measured for chloroform solutions and in thin solid films (Figure 1), and the corresponding data are listed (Table 1). As seen from Figure 1 and Table 1, the two title compounds having EDOT moiety displayed an identical maximum absorption wavelength (λ_{abs}^{max}) of 519 nm, which is 31 nm red-shifted when compared to the reference compound **COOP-3HT-BDT** ($\lambda_{abs}^{max} = 488$ nm). Such a bathochromic absorption shift can be ascribed to the electron-donating nature of the EDOT unit and better planarity of the molecule.[16] Although the two EDOT-containing compounds show identical λ_{abs}^{max}, compound **COOP-2HT-EDOT-BDT** shows a broader absorption band with a longer absorption onset wavelength λ_{abs}^{onset} of 628 nm and a higher molar extinction coefficient (ε_{abs}^{max}) of 1.06×10^5 L mol^{-1} cm^{-1}, when compared with those of **COOP-EDOT-2HT-BDT** ($\lambda_{abs}^{onset} = 610$ nm, $\varepsilon_{abs}^{max} = 0.96 \times 10^5$ L mol^{-1} cm^{-1}), indicating that the position of the EDOT within the molecule has certain influence on the optical properties of the materials (Figure 1a). In addition, the large red-shifts in thin solid films compared with their chloroform solution (Figure 1b) can be ascribed to intensive π–π interaction in the solid films.[17] Interestingly, no obvious difference was found for the absorption spectra of these three compounds in solid films. Since the absorption spectrum of organic materials in thin solid films is related more to the intermolecular interaction, these results indicate that they have almost similar intermolecular packing behavior in solid films.[18]

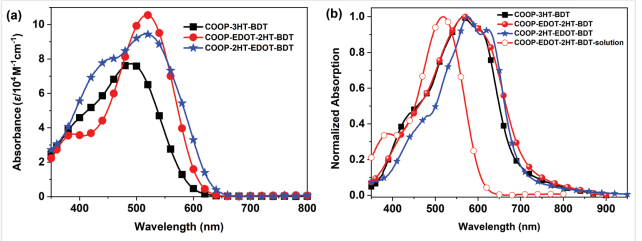

Figure 1 Absorbance spectra of three BDT-cored small molecules in (a) chloroform solution ($c = 1.0 \times 10^{-6}$ mol^{-1}) and (b) thin films.

Electrochemical Properties

Cyclic voltammograms (CVs) of the two target molecules and the reference compound were measured in dilute dichloromethane (Figure 2a), and the corresponding data are summarized in Table 1. As seen here, all these compounds present multiple quasi-reversible oxidation processes in the positive potential range. The first oxidation potentials (E_{ox}^0 vs. Fc^+/Fc) of **COOP-EDOT-2HT-BDT** and **COOP-2HT-EDOT-BDT** were measured to be 0.26 and 0.09 V, respectively, which are lower than that of **COOP-3HT-BDT** (0.50 V). Based on the measured onset oxidation potential (E_{ox}^{onset}), the HOMO energy levels of **COOP-EDOT-2HT-BDT** and **COOP-2HT-EDOT-BDT** were calculated to be −5.26 and −5.08 eV, respectively, which are 0.13 and 0.21 eV higher than that

Table 1 Optical and electrochemical properties of three compounds

Sample	λ_{abs}^{max} (nm)[a]	ε_{abs}^{max} (M^{-1} cm^{-1})[b]	λ_{film}^{max} (nm)	E_g^{opt} (eV)[c]	E_{ox}^0 (V)[d,e]	E_{red}^0 (V)[d,e]	E_{HOMO} (eV)[f]	E_{LUMO} (eV)[f]	E_g^{CV} (eV)[g]
COOP-EDOT-2HT-BDT	519	105,600	568	1.77	0.26	−1.63	−5.26	−3.55	1.71
COOP-2HT-EDOT-BDT	519	94,600	577(624)[h]	1.78	0.09	−1.67	−5.08	−3.52	1.56
COOP-3HT-BDT	488	77,300	564	1.80	0.50	−1.60	−5.39	−3.58	1.81

[a]In $CHCl_3$ (1.0×10^{-6} mol L^{-1}).
[b]Extinction coefficient was obtained by linear fitting absorbance vs. concentration.
[c]Optical band gap, calculated from the absorption onset wavelength (λ_{onset}) in solid film according to the equation E_g^{opt} (eV) = 1240/λ_{onset} (nm).
[d]Measured in CH_2Cl_2 solution (1.0×10^{-3} mol L^{-1}) in a nitrogen atmosphere.
[e]Irreversible wave was estimated as the potential where $i_{pc} = 0.855 \times i_{pc}^{max}$.[19]
[f]Calculated from the cyclic voltammograms, $E_{HOMO} = -[E_{ox}^{onset} + 5.1]$ (eV), $E_{LUMO} = -[E_{red}^{onset} + 5.1]$ (eV).[20]
[g]Electrochemical band gap $E_g^{cv} = E_{LUMO} - E_{HOMO} = E_{ox}^{onset} - E_{red}^{onset}$ (eV).
[h]Shoulder peak.

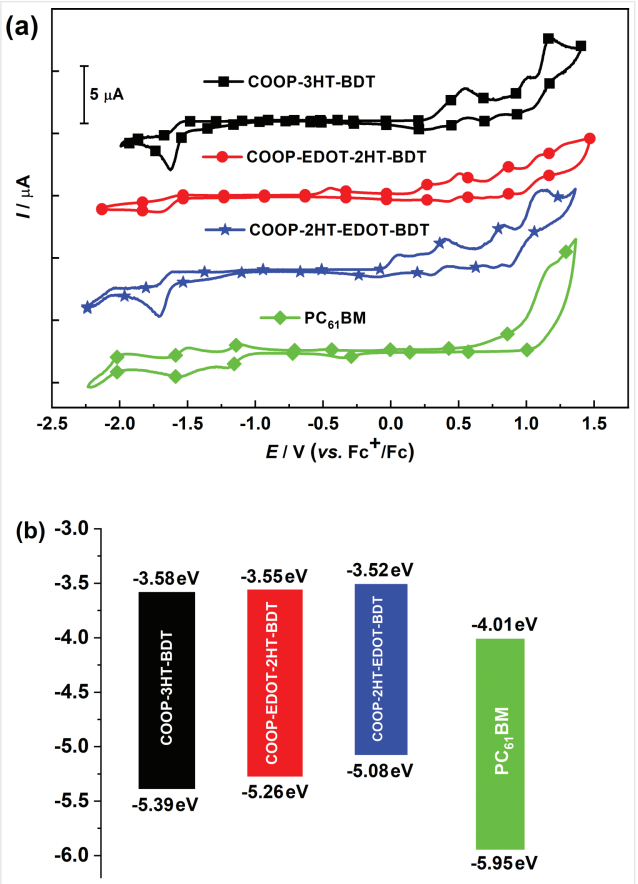

Figure 2 (a) Cyclic voltammograms of three molecules in dry dichloromethane–$TBAPF_6$ (0.1 M), scan speed 100 mV s^{-1}, potentials vs. Fc/Fc^+. (b) HOMO and LUMO energy levels of the molecules.

of **COOP-3HT-BDT** (−5.39 eV). These results indicate that the introduction of the EDOT unit onto the BDT conjugated oligothiophene chain will increase the HOMO energy level, whereby the closer the EDOT unit to the BDT core, the higher HOMO energy level the compound has.

On the other hand, all these three compounds show one irreversible reduction process during a negative potential sweeping with a similar reduction potential ($E_{red}{}^0$) of around −0.60 V (vs. Fc^+/Fc), which can be ascribed to the reduction of identical terminal electron-withdrawing COOP groups.[21] The LUMO energy levels of these three compounds are therefore found to be similar for all these three compounds (between −3.58 eV and −3.52 eV). The band gaps calculated by CV measurement were determined to be 1.71 eV and 1.56 eV for **COOP-EDOT-2HT-BDT** and **COOP-2HT-EDOT-BDT**, which are lower than that of **COOP-3HT-BDT** (1.81 eV).

In short summary, the introduction of electron-donating EDOT unit into the conjugated oligothiophene chain will higher the HOMO energy level and consequently lower the band gap of the final compound. More interestingly, such a substitution effect is more sensitive when EDOT is close to the BDT core, while less impact was found when the EDOT unit is close to the terminal electron acceptor unit.

DFT Calculations

To better understand the effect of the EDOT location on the molecular electronic structure, theoretical calculation was performed for the three compounds using the density functional theory (DFT) method B3LYP with the 6-31G* basis set. All of the alkyl chains were simplified to minimize the calculation cost. As seen in Figure S8 in the Supporting Information, all these molecules show almost co-planar geometries for the π-conjugated BDT–oligothiophene chain. No significant change can be found for the EDOT-involved molecules. Figure 3 depicts the HOMO/LUMO orbitals of these three molecules in the ground state, and the calculated HOMO/LUMO energy levels are listed in Table S1. The calculated electronic wave functions of HOMO are delocalized over the BDT core and two adjacent conjugated units. Owing to the electron-donating nature of the EDOT unit, the HOMO energy level is therefore increased when the EDOT is close to the BDT core. In contrast, when the EDOT unit is far away from the BDT core, the contribution of EDOT to the HOMO orbital is rather weak, which explains why the HOMO energy level is less increased for **COOP-EDOT-2HT-BDT**. The calculated electronic wave functions of LUMO are found to be mainly delocalized over the COOP end-capped acceptor group and the adjacent conjugated thiophene unit would contribute slightly to the LUMO energy level. Therefore, the LUMO energy level is mainly determined by the terminal electron acceptor unit, and a slight variation of LUMO was measured for these EDOT-incorporated conjugated molecules. The theoretical calculation results are in good accordance with the experimental results as listed in Table 1.

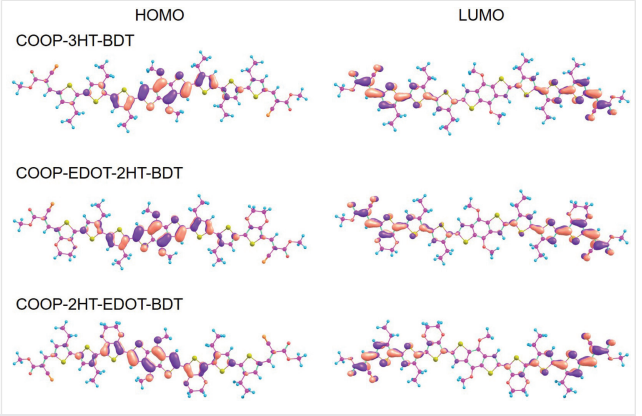

Figure 3 DFT-B3LYP/6-31G* calculated electronic wave functions of the HOMO/LUMO of three related molecules in chloroform solution.

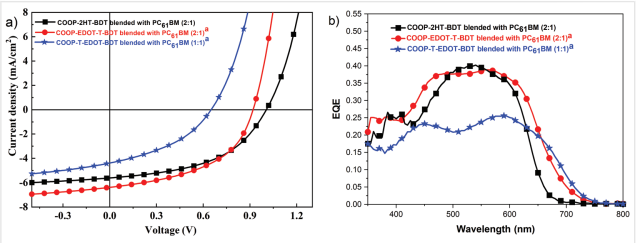

Figure 4 (a) Current density (*J*)–voltage (*V*) curves of devices based on three related donor molecules and $PC_{61}BM$ at best weight ratio. (b) EQE curves of BHJ solar cells based on three related donor molecules and $PC_{61}BM$ at best weight ratio. ([a]Post-annealing at 90 °C for 1 min.)

Photovoltaic Performances

These two title compounds were used as the electronic donor materials for organic solar cells by blended with $PC_{61}BM$ as acceptor materials. Solution-processed bulk heterojunction (BHJ) devices with a conventional structure of indium tin oxide (ITO)/PEDOT:PSS (30 nm)/active layer/LiF (1 nm)/Al (100 nm) were prepared. The optimized conditions of devices for the three compounds are presented (Figure 4a and Table 2). Optimization of the device performance by varying the donor:acceptor blend ratio was performed, and the results are summarized in Tables S2 and [S3] in the Supporting Information. The cell based on the reference compound **COOP-3HT-BDT** with $PC_{61}BM$ at 2:1 (w/w) ratio showed a highest PCE of 3.24%, an open-circuit voltage (V_{OC}) of 0.91 V, a short current density (J_{SC}) of 6.84 mA cm^{-2}, and a fill factor (FF) of 0.52. A slightly lower V_{OC} of 0.87 V with a higher J_{SC} of 7.31 mA cm^{-2} and a higher FF (0.62) was achieved for the **COOP-EDOT-2HT-BDT:**$PC_{61}BM$ cell, yielding a higher PCE of 3.90% for the optimized cell. This result indicates that the EDOT unit is able to improve device performance through the increase of J_{SC}. Surprisingly, all of device parameters for the **COOP-2HT-EDOT-BDT:**$PC_{61}BM$ cell are lower than those of the **COOP-EDOT-2HT-BDT:**$PC_{61}BM$ cell, where a V_{OC} of 0.67 V, a J_{SC} of 6.56 mA cm^{-2} and a FF of 0.51 were obtained, yielding an overall PCE of 2.24%.

External quantum efficiency (EQE) spectra of the optimized devices based on these donor materials blended with acceptor $PC_{61}BM$ were also tested (Figure 4b). As seen here, the **COOP-EDOT-2HT-BDT-**based cell showed a broader spectrum response in comparison with **COOP-3HT-BDT**, which is in good accordance with UV-Vis absorption results. For the **COOP-2HT-EDOT-BDT** cell, although the spectrum response is even broader, a lower quantum efficiency was measured, which lowers the J_{SC} value. Nanomorphology of these three different photoactive layers was measured by transmission electron microscopy (TEM), and the results are shown in Figure 5. As seen here, the **COOP-EDOT-2HT-BDT** and **COOP-3HT-BDT** based blend films showed visible nanofibers in the blend film, which is feasible for charge transfer. However, for the **COOP-2HT-EDOT-BDT** blend film, rather clusters can be found for the blend film. The unfavorable nanomorphology could be one of the reasons for the lower device performance.

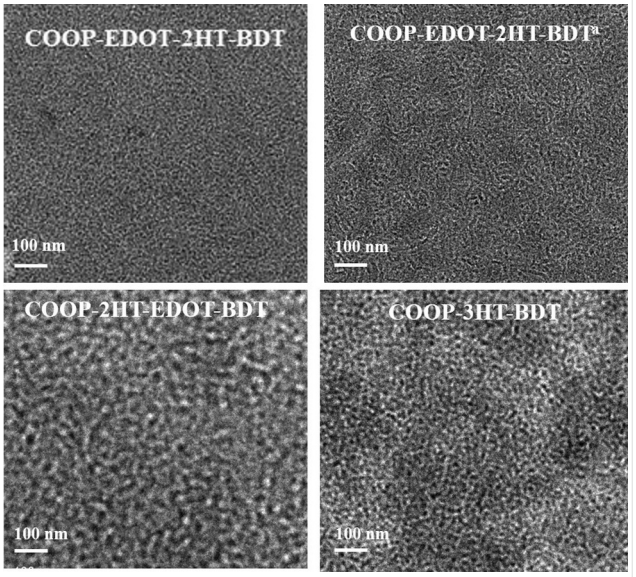

Figure 5 TEM images (scale label 100 nm) of BHJ solar cells based on best devices of three donor molecules blended with $PC_{61}BM$. ([a]Annealing at 90 °C for 1 min.)

With the rapid development of high-performance non-fullerene acceptors for use in polymer solar cells, [22] high PCEs of over 18% were achieved.[23] Conjugated small molecules were reported for use in ternary solar cells.[24] These compounds are also interesting for use in the ternary solar cells, which is under investigation at the current moment.

Table 2 Photovoltaic property data of donor:$PC_{61}BM$-based best devices

Donor	Thickness (nm)	V_{OC} (V)	J_{SC} (mA cm^{-2})[b]	FF (%)	PCE (%)	
					Best	Ave (±std. dev.)[c]
COOP-3HT-BDT	113 ± 5	0.91	6.84	52	3.24	3.14 (±0.15)
COOP-EDOT-2HT-BDT[a]	109 ± 5	0.87	7.31	62	3.90	3.83 (±0.11)
COOP-2HT-EDOT-BDT	102 ± 5	0.67	6.56	51	2.24	2.17 (±0.11)

[a]Post-annealing at 90 °C for 1 min.
[b]Determined by convoluting the spectral response with the AM 1.5G spectrum (100 mW cm^{-2}).
[c]Standard deviation was calculated over 8 individual devices.

Conclusions

In summary, we have synthesized and characterized two novel molecules including **COOP-EDOT-2HT-BDT** and **COOP-2HT-EDOT-BDT** with EDOT moiety in different positions with octyl cyanoacetate terminal group and BDT core. Obvious bathochromic shifts and stronger absorption peaks of optical spectra were found in chloroform solution compared with **COOP-3HT-BDT**. The EDOT unit can also narrow band gaps and increase energy levels of molecular orbitals, and calculated data of wave functions support this result. We obtained the best device performance of **COOP-EDOT-2HT-BDT** with a PCE of 3.90% using BHJ solution process. Furthermore, the experimental results indicated that the position of the electron-donating EDOT moiety plays a significant role in influencing device performances. Our results indicate that placing the electron donating moiety next to the electron acceptor moiety is helpful in achieving high device performance.

Experimental Section

Materials

All the chemical reactions were carried out under a N_2 atmosphere. Organic solvents were purified and dried by the usual methods before the use. Chemicals were purchased and used without further purification: $Pd_2(dba)_3{\cdot}CHCl_3$ (Sigma-Aldrich), $HP(t\text{-}Bu)_3{\cdot}BF_4$ (Sigma-Aldrich), octyl 2-cyanoacetate (Energy Chemical), $Pd(PPh_3)_4$ (Energy Chemical), NBS (Energy Chemical), AcOH (Sinopharm Chemical Reagent Co., Ltd.), K_2CO_3 (Sinopharm Chemical Reagent Co., Ltd.), piperidine (Sinopharm Chemical Reagent Co., Ltd.), 1,1'-[4,8-bis[(2-ethylhexyl) oxy]benzo[1,2-*b*:4,5-*b*']dithiophene-2,6-diyl]bis[1,1,1-trimethylstannane] (**BDT-Sn**, Derthon Optoelectronic Materials Science & Technology Co., Ltd.), *n*-BuLi (J&K Scientific Co., Ltd.), Me_3SnCl (J&K Scientific Co., Ltd.), poly (3,4-ethylenedioxythiophene:poly(styrenesulfonate)) (PEDOT:PSS, Heraeus Precious Metals GmbH & Co. KG.), [6,6]-phenyl-C_{61}-butyric acid methyl ester ($PC_{61}BM$, Solarmer Materials (Beijing) Inc.), [6,6]-phenyl-C_{71}-butyric acid methyl ester ($PC_{71}BM$, Solenne B. V.). **EDOT-Bp**,[12] **CHO-2HT-Br**,[13a13b] **CHO-EDOT-Br**[14] and **Sn-HT**[15] were synthesized according to the literature.

Measurements and Characterization

Nuclear magnetic resonance spectra were recorded on a *Bruker* Avance III 400 spectrometer (^1H NMR: 400 MHz, ^{13}C NMR: 100 MHz). δ values (ppm) with tetramethylsilane as the internal standard to report chemical shifts. Singlet (s), doublet (s), triplet (t) and m (multiplet) are designed to show splitting patterns. Matrix-assisted laser desorption ionization time-of-flight mass spectrometry (MALDI-TOF-MS) spectra were recorded on a Bruker Autoflex Speed spectrometer using *trans*-2-[3-(4-*tert*-butylphenyl)-2-methyl-2-propenylidene] malononitrile (DCTB) as the matrix. Electrospray ionization time-of-flight high-resolution spectrometry (ESI-TOF-MS) was recorded on a *Bruker* micrOTOF-Q III spectrometer. Thermal gravimetric analysis was tested on a Netzsch STA 449 F3 instrument under purified nitrogen gas flow with a 10 °C min^{-1} heating. Optical measurements were recorded on a PerkinElmer Lambda750 instrument. For UV-vis absorption spectrum measurement in chloroform solution, three concentrated solutions (around 10^{-3} mol·L^{-1}) were prepared independently, each of which was further diluted to get three new concentration solutions (with concentration around 10^{-7}–10^{-5} mol·L^{-1}). The absorption spectra of the diluted solutions were recorded, and the data points of the absorbance at a certain maximum absorption wavelength vs. concentration were then plotted. A good linear relationship was found for all these compounds, suggesting that no obvious intermolecular interaction occurred within such concentration range. The molecular molar extinction coefficient (ε) was obtained from the slope of the linear regression equation (best-fit line) over the above-mentioned data points according to the Beer–Lambert's law equation, $A = \varepsilon{\cdot}L{\cdot}c$. Thin solid films for absorption spectra tests were obtained by spin-coating from chloroform solution (ca. 6 mg·mL^{-1}) on cleaned quartz at 2500 rpm. CV was measured in diluted CH_2Cl_2 solution (ca. 1.0×10^{-3} mol/L) in a nitrogen atmosphere at room temperature using tetrabutylammonium hexafluorophosphate (Bu_4NPF_6, 0.1 mol·L^{-1}) as the supporting electrolyte. A RST3000 electrochemical workstation (Suzhou Risetech Instrument Co., Ltd) was operated at a scanning rate of 100 mV s^{-1} for electrochemical study. A Pt wire (ϕ = 1.0 mm) embedded in Teflon column was used as the working electrode, a Pt sheet was used as the counter electrode and Ag/AgCl electrodes were served as the reference electrodes. All potentials were internally referenced to the ferrocene/ferrocenium couple (−5.1 eV vs. vacuum). TEM was taken from an FEI Tecnai G2 F20 S-Twin 2000 kV microscope.

Device Fabrication and Tests

The devices were fabricated with a conventional structure of ITO/ PEDOT: PSS (30 nm)/active layer/LiF (1 nm)/Al (100 nm). We cleaned the ITO glass substrates via ultrasonic treatment successively in detergent, deionized water, acetone, and isopropyl alcohol under ultrasonication for 30 min each. And they were dried by a pure nitrogen blow before the use. After routine solvent cleaning, the ITO substrates were treated with UV ozone for 30 min. PEDOT: PSS (Clevios P VP AI

4083, filtered through 0.45 µm) was spin-coated at 3500 rpm for 1 min to prepare a 30 nm film. The substrates were baked at 124 °C for 10 min in a glove box. Then, donor–acceptor blended chloroform solutions with different ratios were spin-coated to prepare the active layers. Then, the counter electrode of LiF (1.0 nm) and Al (100 nm) was deposited onto the active layer under vacuum (pressure $<1 \times 10^{-4}$ Pa) through a shadow mask. The active areas of the devices were independent 0.16 cm^2 or 0.09 cm^2. No solar cell performance dependence on active area was observed. An AlphaStep profilometer (Veeco, Dektak 150) instrument was used to study film thickness. A Keithley 2400 source meter under an AM 1.5G filter (100 mW·cm^{-2}), which was generated by white light from a tungsten halogen lamp, filtered by a Schott GG385 UV filter and a Hoya LB120 daylight filter, was used for investigation of the current density–voltage (*J*–*V*) characteristics in a nitrogen atmosphere. EQEs were measured under simulated 1 sun operation condition from a 150 W tungsten halogen lamp (Osram 64610) using bias light from a 532 nm solid state laser (Changchun New Industries, MGL-III-532). And light was modulated with a mechanical chopper before passing the monochromator (Zolix, Omni-λ300) to select the wavelength. The response was recorded as the voltage by an *I*–*V* converter (DNR-IV Convertor, Suzhou D&R Instruments), using a lock-in amplifier (Stanford Research Systems SR 830) and a calibrated Si cell as a reference. The device for EQE measurement was kept behind a quartz window in a nitrogen-filled container all the time when tested.

Synthesis

CHO-2HT-EDOT

A solution of compound **CHO-2HT-Br** (5.00 g, 11.34 mmol), **EDOT-Bp** (2.53 g, 9.45 mmol), $Pd_2(dba)_3{\cdot}CHCl_3$ (196 mg, 0.19 mmol) and $HP(t\text{-}Bu)_3{\cdot}BF_4$ (110 mg, 0.38 mmol) in THF (90 mL) was degassed by bubbling N_2 for 15 min. N_2-degrassed K_2CO_3 deionized water solution (1.0 M, 30 mL, 30 mmol) was added and the resulting solution was stirred at room temperature overnight under a N_2 atmosphere. The solution was extracted with $CHCl_3$ after THF was taken off. The organic layer was dried over $MgSO_4$ and the solvent was removed in vacuo. The crude product was purified by flash chromatography (silica gel, *n*-hexane:ethyl acetate = 5:1) to give compound **CHO-2HT-EDOT** (3.46 g, 88% yield) as a pale yellow solid. ^{1}H NMR ($CDCl_3$, 400 MHz): δ = 9.81 (s, 1 H), 7.58 (s, 1 H), 7.11 (s, 1 H), 6.41 (s, 1 H), 4.32–4.24 (m, 4 H), 2.81 (t, J = 8.0 Hz, 2 H), 2.71 (t, J = 8.0 Hz, 2 H), 1.71–1.57 (m, 4 H), 1.38–1.26 (m, 12 H), 0.91–0.86 (m, 6 H). ^{13}C NMR (100 MHz, $CDCl_3$): δ = 182.53, 141.62, 141.51, 140.31, 140.06, 139.91, 139.08, 138.52, 133.52, 129.86, 129.56, 109.58, 99.54, 64.89, 64.44, 31.62, 31.56, 30.39, 30.30, 30.24, 30.20, 29.39, 29.36,29.20, 29.11, 22.56, 14.07. HRMS (ESI-TOF): calcd. for $C_{27}H_{34}O_3S_3$ $[M + H]^+$, 503.1743; found, 503.1741.

CHO-2HT-EDOT-Br

N-Bromosuccinimide (433 mg, 2.43 mmol) was dissolved in 50 mL THF and added dropwise into a solution of **CHO-2HT-EDOT** (1.20 g, 2.39 mmol) and ice acetic acid (2 mL) in THF (100 mL) at 0 °C in the dark. After being stirred for 2 h, the reaction mixture was poured into water (100 mL) and extracted with CH_2Cl_2 after THF was taken off. The organic layer was washed with brine, and then dried over $MgSO_4$. After removal of the solvent, it was chromatographed on silica gel (*n*-hexane:ethyl acetate = 9:1) to afford **CHO-2HT-EDOT-Br** (1.27 g, 92%) as a red solid. ^{1}H NMR ($CDCl_3$, 400 MHz): δ = 9.82 (s, 1 H), 7.58 (s, 1 H), 7.10 (s, 1 H), 4.34–4.29 (m, 4 H), 2.80 (t, J = 8.0 Hz, 2H), 2.68 (t, J = 7.6 Hz, 2H), 1.70–1.61 (q, J = 8.0 Hz, 4 H), 1.35–1.30 (m, 12 H), 0.89 (t, J = 6.8 Hz, 6 H). ^{13}C NMR (100 MHz, $CDCl_3$): δ = 182.52, 141.74, 141.26, 140.21, 140.06, 139.89, 139.03, 137.84, 133.96, 129.48, 128.69, 109.66, 87.41, 64.87, 64.80, 31.60, 31.55, 30.34, 30.23, 29.38, 29.35, 29.16, 29.09, 22.56, 14.06, 14.04. MS (MALDI-TOF): calcd. for $C_{27}H_{33}BrO_3S_2$ $[M]^+$, 580.08; found, 580.71.

COOP-2HT-EDOT-Br

Octyl 2-cyanoacetate (264 mg, 1.34 mmol) was added to a solution of **CHO-2HT-EDOT-Br** (519 mg, 0.89 mmol) and piperidine (0.1 mL) in dry $CHCl_3$ (15 mL) and then the solution was stirred for 6 h under N_2 at 60 °C. Water was added and the reaction mixture was extracted with $CHCl_3$; the combined extracts were washed three times with brine and then dried ($MgSO_4$). The solvent was evaporated under reduced pressure and the crude product further purified by flash chromatography (silica gel, *n*-hexane:$CHCl_3$ = 4:1) to afford a dark red powder (625 mg, 92%). ^{1}H NMR ($CDCl_3$, 400 MHz): δ = 8.19 (d, J = 0.4 Hz, 1 H), 7.56 (s, 1 H), 7.15 (s, 1 H), 4.35–4.31 (m, 4 H), 4.29 (t, J = 6.4 Hz, 2 H), 2.80 (t, J = 8.0 Hz, 2 H), 2.69 (t, J = 7.6 Hz, 2 H), 1.78–1.70 (q, J = 6.8 Hz, 2 H), 1.69–1.60 (m, 4 H), 1.41–1.28 (m, 22 H), 0.91–0.87 (m, 9 H). ^{13}C NMR (100 MHz, $CDCl_3$): δ = 163.17, 146.06, 142.07, 141.78, 140.95, 140.34, 139.94, 137.92, 133.65, 132.78, 129.87, 129.32, 116.03, 109.78, 97.43, 87.55, 66.51, 64.90, 64.83, 31.75, 31.61, 31.54, 30.41, 30.12, 29.48, 29.27, 29.24, 29.15, 29.13, 28.55, 25.78, 22.62, 22.59, 22.58, 14.08, 14.04. MS (MALDI-TOF): calcd. for $C_{38}H_{50}BrNO_4S_3$ $[M]^+$, 759.21; found, 759.12. HRMS (ESI-TOF): calcd. for $C_{38}H_{50}BrNO_4S_3$ $[M + H]^+$, 760.2158; found, 760.2152.

COOP-2HT-EDOT-BDT

A mixture of **COOP-2HT-EDOT-Br** (466 mg, 0.61 mmol), **BDT-Sn** (215 mg, 0.28 mmol), and $Pd(PPh_3)_4$ (35 mg, 27.8 µmol) was stirred at 80 °C in dry DMF (5 mL) for 24 h. After cooled to room temperature, the reaction mixture was added dropwise to anhydrous methanol (15 mL) and stirred for 0.5 h at room temperature. A dark red solid was obtained

by filtering through a Büchner funnel. The residue was purified through thin layer chromatography (silica gel, *n*-hexane:$CHCl_3$ = 2:5) to give a black powder (322 mg, 64%). ^{1}H NMR ($CDCl_3$, 400 MHz): δ = 8.20 (s, 2 H), 7.62 (s, 2 H), 7.57 (s, 2 H), 7.19 (s, 2 H), 4.45 (d, J = 9.2 Hz, 8 H), 4.29 (t, J = 6.8 Hz, 4 H), 4.20 (d, J = 5.2 Hz, 4 H), 2.85–2.81 (m, 8 H), 1.87–1.82 (m, 2 H), 1.79–1.59 (m, 20 H), 1.43–1.25 (m, 52 H), 1.06 (t, J = 7.6 Hz, 6 H), 0.98 (t, J = 6.8 Hz, 6 H), 0.92–0.87 (m, 18 H). ^{13}C NMR (100 MHz, $CDCl_3$): δ = 163.22, 146.00, 143.81, 142.34, 141.32, 141.08, 140.20, 138.61, 138.55, 133.43, 133.33, 132.61, 131.98, 130.08, 129.20, 116.10, 115.78, 112.14, 109.12, 97.09, 75.77, 66.48, 64.92, 40.64, 31.78, 31.65, 31.57, 30.51, 30.41, 30.09, 29.79, 29.68, 29.36, 29.32, 29.22, 29.17, 29.14, 28.55, 25.79, 23.85, 23.17, 22.63, 14.23, 14.11, 14.08, 11.35. MS (MALDI-TOF): calcd. for $C_{102}H_{136}N_2O_{10}S_8$ $[M]^+$, 1804.80; found, 1805.19. HRMS (ESI-TOF): calcd. for $C_{102}H_{136}N_2O_{10}S_8$ $[M + H]^+$, 1805.8039; found, 1805.8015.

CHO-EDOT-HT

A mixture of **CHO-EDOT-Br** (4.00 g, 16.06 mmol), **Sn-HT** (6.40 g, 19.33 mmol), and $Pd(PPh_3)_4$ (928 mg, 0.80 mmol) was stirred at 80 °C in dry DMF (70 mL) for 24 h. After cooled to room temperature, the solvent DMF was removed in vacuo. Then, the mixture was extracted with $CHCl_3$ and deionized water. The organic layer was dried over $MgSO_4$ and the solvent was removed in vacuo. The residue was purified by flash chromatography (SiO_2, *n*-hexane:ethyl acetate = 5:1) to give a pale yellow powder (5.15 g, 95%). ^{1}H NMR ($CDCl_3$, 400 MHz): δ = 9.88 (s, 1 H), 7.25 (s, 1 H), 6.95 (s, 1 H), 4.39 (s, 4 H), 2.58 (t, J = 7.2 Hz, 2 H), 1.64–1.57 (q, J = 6.8 Hz, 2 H), 1.35–1.30 (m, 6 H), 0.88 (t, J = 6.4 Hz, 3 H). ^{13}C NMR (100 MHz, $CDCl_3$): δ = 179.29, 145.58, 143.92, 136.62, 132.98, 127.19, 123.75, 121.84, 114.54, 65.25, 64.73, 31.61, 30.35, 30.30, 28.90, 22.57, 14.05. HRMS (ESI-TOF): calcd. for $C_{17}H_{20}O_3S_2$ $[M + H]^+$, 337.0927; found, 337.0921.

CHO-EDOT-HT-Br

N-Bromosuccinimide (2.50 g, 14.04 mmol) was dissolved in 30 mL THF and added dropwise into a solution of **CHO-EDOT-T-C6** (4.50 g, 13.37 mmol) in THF (100 mL) at −20 °C in the dark. After being stirred for 4 h, the reaction mixture was poured into water (100 mL) and extracted with CH_2Cl_2 after THF was taken off. The organic layer was washed with brine, and then dried over $MgSO_4$. After removal of the solvent, it was chromatographed on silica gel (*n*-hexane:ethyl acetate = 5:1) and recrystallized using ethanol to afford **CHO-EDOT-HT-Br** (4.81 g, 87%) as a pale yellow solid. ^{1}H NMR ($CDCl_3$, 400 MHz) δ ppm: 9.90 (s, 1 H), 7.07 (s, 1 H), 4.41 (s, 4 H), 2.55 (t, J = 8.0 Hz, 2 H), 1.62–1.55 (q, J = 8.0 Hz, 2 H), 1.38–1.28 (m, 6 H), 0.89 (t, J = 8.0 Hz, 3 H). ^{13}C NMR (100 MHz, $CDCl_3$) δ ppm: 179.30, 148.42, 142.59, 136.88, 132.82, 126.08, 122.54, 121.84, 114.78, 111.46, 65.25, 64.82, 31.55, 29.58, 29.41, 28.83, 22.56, 14.05. MS (MALDI-TOF): calcd. for $C_{17}H_{19}BrO_3S_2$ $[M]^+$, 414.00; found, 415.24.

COOP-EDOT-HT-Br

Octyl 2-cyanoacetate (325 mg, 1.65 mmol) was added to a solution of **CHO-EDOT-HT-Br** (460 mg, 1.10 mmol) and piperidine (0.1 mL) in dry $CHCl_3$ (15 mL) and then the solution was stirred for 6 h under N_2 at 60°C. Water was added and the reaction mixture was extracted with $CHCl_3$, then the combined extracts were washed three times with brine and then dried ($MgSO_4$). The solvent was evaporated under reduced pressure and the crude product further purified by flash chromatography (silica gel, *n*-hexane:CH_2Cl_2 = 1:1) to afford a dark red powder (477 mg, 73%). ^{1}H NMR ($CDCl_3$, 400 MHz): δ = 8.37 (s, 1 H), 7.13 (s, 1 H), 4.41 (s, 4 H), 4.26 (t, J = 8.0 Hz, 2 H), 2.55 (t, J = 8.0 Hz, 2 H), 1.76–1.70 (q, J = 8.0 Hz, 2 H), 1.61–1.58 (m, 2 H), 1.41–1.28 (m, 16 H), 0.90–0.87 (m, 6 H). ^{13}C NMR (100 MHz, $CDCl_3$): δ = 163.53, 148.31, 142.80, 141.21, 136.77, 132.44, 126.48, 122.88, 116.82, 112.57, 109.72, 93.61, 66.21, 65.44, 64.84, 31.74, 31.54, 29.59, 29.41, 29.16, 29.13, 28.88, 28.58, 25.78, 22.62, 22.55, 14.06, 14.05. MS (MALDI-TOF): calcd. for $C_{28}H_{36}BrNO_4S_2$ $[M]^+$, 593.13; found, 593.19. HRMS (ESI-TOF): calcd. for $C_{28}H_{36}BrNO_4S_2$ $[M + H]^+$, 594.1342; found, 594.1339.

HT-BDT-HT

A mixture of **BDT-Sn** (1.50 g, 1.94 mmol), **HT-Br** (1.44 g, 5.83 mmol), and $Pd(PPh_3)_4$ (225 mg, 0.19 mmol) was stirred at 80 °C in dry DMF (6 mL) for 19 h. After cooled to room temperature, the solvent DMF was removed in vacuo. Then, the mixture was extracted with $CHCl_3$ and deionized water. The organic layer was dried over $MgSO_4$ and the solvent was removed in vacuo. The residue was purified by flash chromatography (SiO_2, *n*-hexane) to give a yellow solid (1.26 g, 83%). ^{1}H NMR ($CDCl_3$, 400 MHz): δ = 7.44 (s, 2 H), 7.26 (d, J = 5.2 Hz, 2 H), 6.99 (d, J = 5.2 Hz, 2 H), 4.20 (d, J = 5.2 Hz, 4 H), 2.88 (t, J = 7.6 Hz, 4 H), 1.85–1.79 (q, J = 6.0 Hz, 2 H), 1.76–1.55 (m, 12 H), 1.47–1.35 (m, 12 H), 1.35–1.29 (m, 8 H), 1.03 (t, J = 7.2 Hz, 6H), 0.95–0.92 (t, J = 8.0 Hz, 6 H), 0.90–0.86 (m, 6 H). ^{13}C NMR (100 MHz, $CDCl_3$): δ = 143.93, 140.94, 135.91, 131.82, 130.73, 130.30, 129.80, 124.82, 118.32, 40.65, 31.71, 30.81, 30.48, 29.69, 29.46, 29.31, 29.23, 23.86, 23.12, 22.64, 14.15, 14.07, 11.32. MS (MALDI-TOF): calcd. for $C_{46}H_{66}O_2S_4$ $[M]^+$, 778.39; found, 778.80.

HT-BDT-Sn

n-BuLi (1.7 mL, 3.85 mmol, 2.4 M in *n*-hexane) was dropped into a solution of **HT-BDT-HT** (1.00 g, 1.28 mmol) in THF (10 mL) at −78 °C under a nitrogen atmosphere and

stirred for 30 min. Then the mixture was stirred for additional 30 min at room temperature. A solution of Me_3SnCl (640 mg, 3.21 mmol) in 5 mL of THF was added and the mixture slowly warmed to room temperature and stirred overnight. 10 mL KF solution was added and the reaction mixture was extracted with diethyl ether, and the combined extracts were washed three times with brine and then dried ($MgSO_4$). The solvent was evaporated under reduced pressure to obtain a bright yellow solid and without further purification to use. ^{1}H NMR ($CDCl_3$, 400 MHz): δ = 7.43 (s, 2 H), 7.04 (s, 2 H), 4.19 (d, J = 5.6 Hz, 4 H), 2.89 (t, J = 8.0 Hz, 4 H), 1.85–1.79 (m, 2 H), 1.75–1.56 (m, 12 H), 1.48–1.37 (m, 12 H), 1.35–1.30 (m, 8 H), 1.02 (t, J = 7.6 Hz, 6 H), 0.96–0.92 (m, 6 H), 0.90–0.86 (m, 6 H), 0.40 (s, 18 H).

COOP-EDOT-2HT-BDT

A mixture of **COOP-EDOT-HT-Br** (375 mg, 0.63 mmol), **HT-BDT-Sn** (317 mg, 0.29 mmol), and $Pd(PPh_3)_4$ (33 mg, 28.7 µmol) was stirred at 80 °C in dry DMF (4 mL) for 15 h. After cooled to room temperature, the reaction mixture was added dropwise to anhydrous methanol (15 mL) and stirred for 0.5 h at room temperature. A dark red solid was obtained by filtering through a Büchner funnel. The residue was purified through thin layer chromatography (silica gel, n-hexane:$CHCl_3$ = 1:1) to give a black powder (327 mg, 63%). ^{1}H NMR ($CDCl_3$, 400 MHz): δ = 8.38 (s, 2 H), 7.47 (s, 2 H), 7.31 (s, 2 H), 7.07 (s, 2 H), 4.44 (s, 8 H), 4.28–4.22 (m, 8 H), 2.89 (t, J = 6.8 Hz, 4 H), 2.82 (t, J = 6.0 Hz, 4 H), 1.85–1.81 (m, 2 H), 1.76–1.59 (m, 20 H), 1.43–1.29 (m, 52 H), 1.04 (t, J = 7.2 Hz, 6 H), 0.97–0.87 (m, 24 H). ^{13}C NMR (100 MHz, $CDCl_3$): δ = 163.68, 148.42, 143.94, 141.30, 141.03, 140.32, 136.81, 135.42, 134.62, 133.52, 131.95, 131.41, 130.57, 129.67, 129.45, 129.09, 123.70, 118.10, 117.02, 109.86, 93.08, 66.17, 65.47, 64.87, 40.70, 31.81, 31.78, 31.69, 31.62, 30.67, 30.52, 30.41, 29.73, 29.60, 29.44, 29.37, 29.28, 29.25, 29.21, 28.65, 25.85, 23.89, 23.17, 22.67, 14.19, 14.09, 11.34. MS (MALDI-TOF): calcd. for $C_{102}H_{136}N_2O_{10}S_8$ $[M]^+$, 1804.80; found, 1805.06. HRMS (ESI-TOF): calcd. for $C_{102}H_{136}N_2O_{10}S_8$ $[M + H]^+$, 1805.8039; found, 1805.8041.

Funding Information

Financial support for this project was provided by the National Natural Science Foundation of China (22075315) and by Xi'an Jiaotong-Liverpool University Research Development Fund (RDF-14-02-46).

Acknowledgment

The authors would like to acknowledge the National Natural Science Foundation of China and Xi'an Jiaotong-Liverpool University for the financial support.

Supporting Information

Supporting information for this article is available online at https://doi.org/10.1055/a-1472-7109.

References

(1) (a) Lin, Y.; Zhan, X. *Acc. Chem. Res.* **2016**, *49*, 175. (b) Hou, J.; Inganäs, O.; Friend, R. H.; Gao, F. *Nat. Mater.* **2018**, *17*, 119. (c) Ye, W.; Yang, Y.; Zhang, Z.; Zhu, Y.; Ye, L.; Miao, C.; Lin, Y.; Zhang, S. *Sol. RRL* **2020**, *4*, 2000258. (d) Kan, B.; Kan, Y.; Zuo, L.; Shi, X.; Gao, K. *InfoMat* **2021**, *3*, 175.

(2) (a) Tang, H.; Yan, C.; Huang, J.; Kan, Z.; Xiao, Z.; Sun, K.; Li, G.; Lu, S. *Matter* **2020**, *3*, 1403. (b) Zheng, B.; Huo, L. *Sci. China Chem.* **2021**, *64*, 358.

(3) (a) Min, J.; Cui, C.; Heumueller, T.; Fladischer, S.; Cheng, X.; Spiecker, E.; Li, Y.; Brabec, C. J. *Adv. Energy Mater.* **2016**, *6*, 1600515. (b) Lee, C. J.; Mitchell, V. D.; White, J.; Jiao, X.; McNeill, C. R.; Subbiah, J.; Jones, D. J. *J. Mater. Chem. A* **2019**, *7*, 6312. (c) Subbiah, J.; Lee, C. J.; Mitchell, V. D.; Jones, D. J. *ACS Appl. Mater. Interfaces* **2021**, *13*, 1086.

(4) (a) Qiu, B.; Xue, L.; Yang, Y.; Bin, H.; Zhang, Y.; Zhang, C.; Xiao, M.; Park, K.; Morrison, W.; Zhang, Z.-G.; Li, Y. *Chem. Mater.* **2017**, *29*, 7543. (b) Bin, H.; Yang, Y.; Zhang, Z.-G.; Ye, L.; Ghasemi, M.; Chen, S.; Zhang, Y.; Zhang, C.; Sun, C.; Xue, L.; Yang, C.; Ade, H.; Li, Y. *J. Am. Chem. Soc.* **2017**, *139*, 5085. (c) Duan, T.; Tang, H.; Liang, R.-Z.; Lv, J.; Kan, Z.; Singh, R.; Kumar, M.; Xiao, Z.; Lu, S.; Laquai, F. *J. Mater. Chem. A* **2019**, *7*, 2541.

(5) (a) Wang, L.; Zhang, Y.; Yin, N.; Lin, Y.; Gao, W.; Luo, Q.; Tan, H.; Yang, H.-B.; Ma, C.-Q. *Sol. Energy Mater. Sol. Cells* **2016**, *157*, 831. (b) Wang, K.; Liang, R.-Z.; Wolf, J.; Saleem, Q.; Babics, M.; Wucher, P.; Abdelsamie, M.; Amassian, A.; Hansen, M. R.; Beaujuge, P. M. *Adv. Funct. Mater.* **2016**, *26*, 7103. (c) Wan, J.; Xu, X.; Zhang, G.; Li, Y.; Feng, K.; Peng, Q. *Energy Environ. Sci.* **2017**, *10*, 1739. (d) Huo, Y.; Gong, X.-T.; Lau, T.-K.; Xiao, T.; Yan, C.; Lu, X.; Lu, G.; Zhan, X.; Zhang, H.-L. *Chem. Mater.* **2018**, *30*, 8661. (e) Wu, Q.; Deng, D.; Zhang, J.; Zou, W.; Yang, Y.; Wang, Z.; Li, H.; Zhou, R.; Lu, K.; Wei, Z. *Sci. China Chem.* **2019**, *62*, 837.

(6) Qin, J.; An, C.; Zhang, J.; Ma, K.; Yang, Y.; Zhang, T.; Li, S.; Xian, K.; Cui, Y.; Tang, Y.; Ma, W.; Yao, H.; Zhang, S.; Xu, B.; He, C.; Hou, J. *Sci. China Mater.* **2020**, *63*, 1142.

(7) (a) Roncali, J.; Blanchard, P.; Frère, P. *J. Mater. Chem.* **2005**, *15*, 1589. (b) Wang, Q.; Zeng, Z.; Li, Y.; Chen, X. *Sol. Energy* **2020**, *208*, 10. (c) Ming, S.; Li, Z.; Zhen, S.; Liu, P.; Jiang, F.; Nie, G.; Xu, J. *Chem. Eng. J.* **2020**, *390*, 124572.

(8) Beaujuge, P. M.; Amb, C. M.; Reynolds, J. R. *Acc. Chem. Res.* **2010**, *43*, 1396.

(9) Montcada, N. F.; Domínguez, R.; Pelado, B.; Cruz, P. l.; Palomares, E.; Langa, F. *J. Mater. Chem. A* **2015**, *3*, 11340.

(10) Hwang, Y.-J.; Li, H.; Courtright, B. A. E.; Subramaniyan, S.; Jenekhe, S. A. *Adv. Mater.* **2016**, *28*, 124.

(11) Wu, Y.; Wang, Z.; Liang, M.; Cheng, H.; Li, M.; Liu, L.; Wang, B.; Wu, J.; Prasad Ghimire, R.; Wang, X.; Sun, Z.; Xue, S.; Qiao, Q. *ACS Appl. Mater. Interfaces* **2018**, *10*, 17883.

(12) Trippé-Allard, G.; Lacroix, J.-C. *Tetrahedron* **2013**, *69*, 861.

(13) (a) Cremer, J.; Mena-Osteritz, E.; Pschierer, N. G.; Müllen, K.; Bäuerle, P. *Org. Biomol. Chem.* **2005**, *3*, 985. (b) Weidelener, M.; Wessendorf, C. D.; Hanisch, J.; Ahlswede, E.; Götz, G.; Lindén, M.; Schulz, G.; Mena-Osteritz, E.; Mishra, A.; Bäuerle, P. *Chem. Commun.* **2013**, *49*, 10865.

(14) Jessing, M.; Brandt, M.; Jensen, K. J.; Christensen, J. B.; Boas, U. *J. Org. Chem.* **2006**, *71*, 6734.
(15) Medlej, H.; Awada, H.; Abbas, M.; Wantz, G.; Bousquet, A.; Grelet, E.; Hariri, K.; Hamieh, T.; Hiorns, R. C.; Dagron-Lartigau, C. *Eur. Polym. J.* **2013**, *49*, 4176.
(16) Marques dos Santos, J.; Neophytou, M.; Wiles, A.; Howells, C. T.; Ashraf, R. S.; McCulloch, I.; Cooke, G. *Dyes Pigm.* **2021**, *188*, 109152.
(17) (a) Li, Z.; He, G.; Wan, X.; Liu, Y.; Zhou, J.; Long, G.; Zuo, Y.; Zhang, M.; Chen, Y. *Adv. Energy Mater.* **2012**, *2*, 74. (b) Long, G.; Wan, X.; Kan, B.; Liu, Y.; He, G.; Li, Z.; Zhang, Y.; Zhang, Y.; Zhang, Q.; Zhang, M.; Chen, Y. *Adv. Energy Mater.* **2013**, *3*, 639.
(18) (a) Yao, Z.-F.; Wang, J.-Y.; Pei, J. *Cryst. Growth Des.* **2018**, *18*, 7. (b) Li, Y.; Lee, D. H.; Lee, J.; Nguyen, T. L.; Hwang, S.; Park, M. J.; Choi, D. H.; Woo, H. Y. *Adv. Funct. Mater.* **2017**, *27*, 1701942.
(19) (a) Ma, C.-Q.; Mena-Osteritz, E.; Wunderlin, M.; Schulz, G.; Bäuerle, P. *Chem. Eur. J.* **2012**, *18*, 12880. (b) Adams, R. N. Electrochemistry at Solid electrode. Marcel Dekker, Inc.: New York, **1969**.
(20) Cardona, C. M.; Li, W.; Kaifer, A. E.; Stockdale, D.; Bazan, G. C. *Adv. Mater.* **2011**, *23*, 2367.
(21) Yin, N.; Wang, L.; Lin, Y.; Yi, J.; Yan, L.; Dou, J.; Yang, H.-B.; Zhao, X.; Ma, C.-Q. *Beilstein J. Org. Chem.* **2016**, *12*, 1788.
(22) (a) Yan, C.; Barlow, S.; Wang, Z.; Yan, H.; Jen, A. K. Y.; Marder, S. R.; Zhan, X. *Nat. Rev. Mater.* **2018**, *3*, 18003. (b) Wadsworth, A.; Moser, M.; Marks, A.; Little, M. S.; Gasparini, N.; Brabec, C. J.; Baran, D.; McCulloch, I. *Chem. Soc. Rev.* **2019**, *48*, 1596. (c) Meredith, P.; Li, W.; Armin, A. *Adv. Energy Mater.* **2020**, *10*, 2001788.
(23) (a) Liu, Q.; Jiang, Y.; Jin, K.; Qin, J.; Xu, J.; Li, W.; Xiong, J.; Liu, J.; Xiao, Z.; Sun, K.; Yang, S.; Zhang, X.; Ding, L. *Sci. Bull.* **2020**, *65*, 272. (b) Zhang, M.; Zhu, L.; Zhou, G.; Hao, T.; Qiu, C.; Zhao, Z.; Hu, Q.; Larson, B. W.; Zhu, H.; Ma, Z.; Tang, Z.; Feng, W.; Zhang, Y.; Russell, T. P.; Liu, F. *Nat. Commun.* **2021**, *12*, 309.
(24) Bi, P.; Hao, X. *Sol. RRL* **2019**, *3*, 1800263.